HIGH-SPEED ISOTACHOPHORESIS. ANALYTICAL ASPECTS OF THE STEADY-STATE LONGITUDINAL TEMPERATURE PROFILES

Zbyněk Ryšlavý*, Petr Boček, Miroslav Deml and Jaroslav Janák
Institute of Analytical Chemistry,
Czechoslovak Academy of Sciences, 662 28 Brno

Received June 26th, 1978

Dedicated to Professor F. Čůta on the occasion of his 80th birthday.

The problem of the longitudinal temperature distribution was solved and the bearing of the temperature profiles on the qualitative characteristics of the zones and on the interpretation of the record of the separation obtained from a universal detector was considered. Two approximative physical models were applied to the solution: in the first model, the temperature dependences of the mobilities are taken into account, the continuous character of the electric field intensity at the boundary being neglected; in the other model, the continuous character of the electric field intensity is allowed for. From a comparison of the two models it follows that in practice, the variations of the mobilities with the temperature are the principal factor affecting the shape of the temperature profiles, the assumption of a discontinuous jump of the electric field intensity at the boundary being a good approximation to the reality. It was deduced theoretically and verified experimentally that the longitudinal profiles can appreciably affect the longitudinal variation of the effective mobilities in the zone, with an infavourable influence upon the qualitative interpretation of the record. Pronounced effects can appear during the analyses of the minor components, where in the corresponding short zone a temperature distribution occurs due to the influence of the temperatures of the neighbouring zones such that the temperature in the zone of interest in fact does not attain a constant value in axial direction. The minor component does not possess the steady-state mobility throughout the zone, which makes the identification of the zone rather difficult.

The different production of heat in successive zones is a characteristic feature of isotachophoretic separation, as has been described by Kendall[1]. This results in longitudinal temperature gradients in the boundary regions and stepwise increase of temperature in the individual zones. In the development of the method the differences in the temperatures of the zones have played an important part, since monitoring of the temperature represented the first universal analytically applicable and sufficiently sensitive detection principle in the analytical capillary isotachophoresis[2,3]. As the detection with thermocouples came into use, attention was paid to the longitudinal temperature distribution[4–7].

* Present address: Central Geochemical Laboratory, Stráž pod Rálskem.

At present, the significance of the thermocouple detector has dropped, the temperature aspects of the isotachophoretic method, however, continue to draw attention. The existence of the temperature dependence of the effective mobilities gives rise to many problems which have to be solved for the analytical capillary isotachophoresis. In current working conditions, the temperature differences between the zones may exceed 10°C, which, regarding the pronounced temperature dependence of the mobilities (approximately 2% per 1°C), has a bearing on the separation and on the analytical interpretation of the isotachophoregrams[8]. Attention has been paid to the problem of the influence of the electric current on the increase of temperature within long zones[9], to the effect of the thermostating temperature on the separation[10], and to the consequences of the different mean zone temperatures for the qualitative interpretation of the isotachophoretic record[8]. The question of the radial and transversal temperature profiles has been treated as well[9,11–15].

So far, however, the longitudinal temperature distribution has not been sufficiently studied as far as the mutual influencing of the neighbouring zones is concerned. This aspect is of particular importance especially in the case of analysis of the minor sample components, forming short zones. In fact, the temperature – and thus the effective mobility – can be markedly affected by the encompassing zones; and in the case of very short zones it may happen that the temperature within the zone is not constant along the column axis. The effective mobility within the zone is then variable, and the corresponding wave in the record does not possess a constant height. This effect depends upon the composition of the sample analyzed. The infavourable consequences of such a phenomenon for the analysis are evident. In order that we may be able to appraise its significance, we assess in this work the axial distribution of temperature and examine how the profiles are affected by the boundary width and the temperature dependence of the conductivity.

THEORETICAL

Inside an isotachophoretic column of a circular cross section, radial temperature gradients establish. The difference between the temperatures in the centre and at the inner wall of the capillary column can be neglected[15] relative to the increase of the mean temperature in the zone for current column diameters[16] and working conditions. Under this assumption, the following approximative physical models can be applied: Due to the passage of the electric current the zones are heated and the heat is removed by the surroundings. Inside a long zone, a steady state is attained, and a mean radially independent temperature occurs within the zone. At the interface of two zones, however, the dissipation of energy changes, which gives rise to longitudinal temperature gradients.

For a volume element inside an isotachophoretic column of a circular cross section, the energy conservation equation can be written assuming that $\mathrm{d}T/\mathrm{d}r = 0$:

$$Sk_1(\partial^2 T/\partial x^2)\,\mathrm{d}x - F_0\,\mathrm{d}x + P\,\mathrm{d}x - SU\varrho C\,\mathrm{d}T = S\,\mathrm{d}x C_\varrho - \mathrm{d}T/\mathrm{d}\tau\,; \qquad (1)$$

here F_0 is the radial heat flux through the column wall along a unit column length and T is the mean temperature in the zone, U is the zone travel velocity, ϱ is the density of the medium possessing the specific heat C and heat conductivity k_1, S is the column cross section, and P is the power dissipated along a unit length of the column.* F_0 can be expressed[17] as

$$F_0 = (T - T_0)/[Q(R_1)]\,, \qquad (2)$$

where

$$Q(R_1) = (1/2\pi k_2)\left[\ln(R_2/R_1) + (k_2/HR_2)\right]. \qquad (3)$$

From Eqs (*1*)–(*3*), the equation of the steady-state temperatures along the column axis can be set up:

$$(\mathrm{d}^2T/\mathrm{d}x^2) - m(\mathrm{d}T/\mathrm{d}x) - \beta(T - T_0) + \beta QP = 0\,, \qquad (4)$$

where

$$m = U\varrho C/k_1 \qquad (5)$$

$$\beta = (QSk_1)^{-1}\,. \qquad (6)$$

The quantity Q, which has been defined in[9], represents the increase of the mean temperature resulting from the dissipation of the power P along a unit length, and its value can be either calculated based on the material and geometrical data (see[9,11–14]) or measured[9,15]. The boundary between the zones has the character of a phase interface, where the concentrations of the components, the electric conductivity, and the electric field intensity change continuously, but very rapidly. These quantities affect each other *via* the temperature dependence of the mobilities, the temperature in a site being governed by the produced heat power.

The change of the power P at the boundary is determined by two factors: *1*) The change of the electric field intensity at the boundary due to the nonzero width of the concentration boundary. *2*) The change of the field intensity at the boundary due to the temperature dependence of the mobilities. The former factor is more significant for lower currents, in which case the voltage gradient and the energy dissipation are small and due to the lower voltage gradient the concentration boundary width is greater (the ion focusation is poorer). The boundary width also increases if the difference between the effective mobilities in the two zones is lowered[18]. The second factor becomes more significant when a higher driving current is applied and the difference

* See also the appended List of Symbols.

between the electric field intensities in the two zones rises. This effect favours the zone sharpening and brings about a lowering of the boundary width. As the driving current increases, the dissipation of energy is higher, the temperature gradients at the boundary grow considerably, and consequently a range of variable effective mobilities forms inside the zone of a component. This effect shows up in the detector response in the range of the boundary.

The mathematical description of the two effects simultaneously reduces to nonlinear differential equations difficult to solve; the solution of a general case of this type is not known. For practical purposes, it is convenient to treat this problem approximatively by employing two different models, based on different assumptions concerning the behaviour of the electric power at the boundary and its temperature dependence.

The Power at the Zone Boundary Has a Continuous Character and is Temperature Independent

This model suits for low differences between the effective mobilities in the neighbouring zones, if the separation is carried out with low currents implying low migration velocities. The limit case is represented by so called concentration boundary, which contains the same number of species on both sides and migration velocity of which is very low[19]. The differences of the mobilities on the two sides of the interface are naturally negligible. The behaviour of the electric field – and consequently of the power – can be then expressed by a continuous function of the sigmoid form[18]. This can be approximated for the two neighbouring zones by two exponentials of the form

$$P_1 = P_1^0 + c_1 \exp(r_1 x), \quad r_1, c_1 > 0; x \leqq 0 \tag{7a}$$

$$P_2 = P_2^0 + c_2 \exp(r_2 x), \quad r_2, c_2 < 0; x \geqq b. \tag{7b}$$

The origin of the coordinate system $x = 0$ lies in the point where $P_1 = P_2$. The exponents r_1, r_2 determine the boundary width and by varying them one can model the change of this width. Inserting the system (*7a, b*) in Eq. (*4*) we obtain a system of non-homogeneous second-order linear equations with constant coefficients for the zones 1 and 2 ($i = 1, 2$):

$$(d^2 v_i/dx^2) - m(dv_i/dx) - \beta v_i = c_i \beta Q \exp(r_i x), \tag{8}$$

where

$$v_i = T_i - T_0 - QP_i^0.$$

The solution of this system, regarding the boundedness of the function, is of the form

$$v_i = a_i \exp(\lambda_i x) - (c_i \beta Q / z_i) \exp(r_i x), \tag{9}$$

where

$$\lambda_1 = \tfrac{1}{2}[m + (m^2 + 4\beta)^{1/2}], \tag{10}$$

$$\lambda_2 = \tfrac{1}{2}[m - (m^2 + 4\beta)^{1/2}], \tag{11}$$

$$z_i = (r_i - \lambda_1)(r_i - \lambda_2). \tag{12}$$

The behaviour of the temperature can be expressed *via* the normalized function ξ:

$$\xi_i = [T_i - T_0 - QP_i^0]/[Q(P_2^0 - P_1^0)]. \tag{13}$$

The constants a_i in the system (9) are determined from the conditions of continuity of the function v_i and of its first-order derivative in the origin of the coordinates. In this manner we obtain

$$\xi_1 = \frac{\lambda_2}{\lambda_2 - \lambda_1}\left[1 + \beta\left(\frac{g_1}{z_1} - \frac{g_2}{z_2}\right) - \frac{\beta}{\lambda_2}\left(\frac{g_1 r_1}{z_1} - \frac{g_2 r_2}{z_2}\right)\right]\exp(\lambda_1 x) - \frac{g_1 \beta}{z_1}\exp(r_1 x) \tag{14a}$$

$$\xi_2 = \frac{\lambda_1}{\lambda_2 - \lambda_1}\left[1 + \beta\left(\frac{g_1}{z_1} - \frac{g_2}{z_2}\right) - \frac{\beta}{\lambda_1}\left(\frac{g_1 r_1}{z_1} - \frac{g_2 r_2}{z_2}\right)\right]\exp(\lambda_2 x) - \frac{g_2 \beta}{z_2}\exp(r_2 x) + 1, \tag{14b}$$

where one of the values $g_i = c_i/(P_2^0 - P_1^0)$ can be chosen so that $g_1 - g_2 = 1$. For $r_1 \to \infty$ and $r_2 \to -\infty$ the normalized function takes the form

$$\xi_1 = [\lambda_2/(\lambda_2 - \lambda_1)] \exp(\lambda_1 x) \tag{15a}$$

$$\xi_2 = [\lambda_1/(\lambda_2 - \lambda_1)] \exp(\lambda_2 x) + 1. \tag{15b}$$

This normalized function corresponds to the functions published previously[14], describing the temperature behaviour at the boundary of two zones and set up under the assumption of temperature independent mobilities and for a discontinuous jump of the conductivity at the boundary.

The Power at the Zone Boundary Changes by a Discontinuous Jump and is Temperature Dependent

This model is appropriate for the case of the separation of components with great differences of the effective mobilities using high driving currents implying high migration velocities (high-speed isotachophoresis). At the boundary, the ions are well focused and the electric field jumps rapidly; the power can be approximated by a discontinuous jump function. The high temperature differences within a zone require that the equation describing the power involve also the dependence of the latter on the temperature. The power P obeys the relation[8]

$$P = P^s/[1 + \alpha(T - T_0)] , \qquad (16)$$

where P^s is the theoretical power which would be dissipated in a zone of the temperature T_0 or as if $\alpha = 0$. For a simplification, we replace[11,12] the expression $1/[1 + \alpha(T - T_0)]$ with the term $1 + v(T - T_0)$, which for the temperature interval of interest can be made with a sufficient accuracy[11], and – as will be shown below – the solution can be expressed by means of the coefficients α solely. Inserting Eq. (*16*) in Eq. (*4*) by employing the temperature coefficient v we obtain

$$(d^2w_i/dx^2) - m(dw/dx) - q_i w_i = 0 , \qquad (17)$$

where

$$q_i = \beta(1 - v_i Q P_i^s) , \qquad (18)$$

$$w_i = T_i - T_0 - Q P_i = T_i - T_0 - Q P_i^s/(1 - v_i Q P_i^s) . \qquad (19)$$

Eq. (*17*) is solved taking into account the boundedness of the function and the continuity of both the function and its first-order derivative and can be again expressed in the form of a normalized function defined by Eq. (*13*):

$$\xi_1' = [\omega_2/(\omega_2 - \omega_1)] \exp(\omega_1 x) \qquad (20a)$$

$$\xi_2' = [\omega_1/(\omega_2 - \omega_1)] \exp(\omega_2 x) + 1 , \qquad (20b)$$

where with regard to Eq. (*19*),

$$\omega_1 = \tfrac{1}{2}\{m + [m^2 + 4\beta(1 + \alpha_1 Q P_1^0)]^{1/2}\} \qquad (21)$$

$$\omega_2 = \tfrac{1}{2}\{m - [m^2 + 4\beta(1 + \alpha_2 Q P_2^0)]^{1/2}\} . \qquad (22)$$

The powers P_i^0, *i.e.* the powers dissipated in a sufficient distance from the boundary, where the temperature changes only negligibly, can be found by employing the tabu-

lated values of the ionic mobilities for the thermostating temperature used and for the driving current applied. In fact, from Eq. (*16*) we have

$$P_i^0 = (1/2\alpha_i Q)\left[-1 + (1 + 4\alpha_i Q P_i^s)^{1/2}\right]. \tag{23}$$

By this procedure we can arrive at the temperature profiles based on the tabulated conductivity values, pertaining to the thermostat temperature.

For an assessment of the effect of the boundary diffusion width or of the effect of the temperature dependence of the mobilities on the temperature behaviour at the boundary, it is convenient to describe the temperature distribution in terms of the statistical moments of the function $d\xi/dx$, as has been applied to the characterization of the thermocouple detector response[6,7]. The definition equations of the *n*-th moment and the n-th central moment of a function $f(x)$ are

$$\mu'_n = \frac{\int x^n f(x)\,dx}{\int f(x)\,d(x)}, \tag{24}$$

$$\mu_n = \frac{\int (x - \mu'_1)^n f(x)\,dx}{\int f(x)\,dx} = \sum_{i=1}^{n} \binom{n}{i} (-\mu'_1)^i (\mu'_{n-1}). \tag{25}$$

For the moments of the derivatives of the function given by Eq. (*9*) we have

$$\mu'_1 = \left[\left(\frac{a_2}{\lambda_2} - \frac{a_1}{\lambda_1}\right) + \beta\left(\frac{g_1}{z_1 r_1} - \frac{g_2}{z_2 r_2}\right)\right], \tag{26}$$

$$\mu'_2 = 2\left[\left(\frac{a_1}{\lambda_1^2} - \frac{a_2}{\lambda_2^2}\right) - \beta\left(\frac{g_1}{z_1 r_1^2} - \frac{g_2}{z_2 r_2^2}\right)\right]. \tag{27}$$

The second central moment can be obtained from Eqs (*26*)–(*27*) by summation in the sense of Eq. (*25*). The second central moment of the derivative of the function ξ (Eq. (*15a, b*)) is

$$\mu_2 = \frac{2}{\lambda_2 - \lambda_1}\left(\frac{\lambda_2}{\lambda_1^2} - \frac{\lambda_1}{\lambda_2^2}\right) - \frac{1}{(\lambda_2 - \lambda_1)^2}\left(\frac{\lambda_1}{\lambda_2} - \frac{\lambda_2}{\lambda_1}\right)^2. \tag{28}$$

This applies also to the function ξ' (Eq. (*20a, b*)), if the coefficients λ_i are replaced by the coefficients ω_i.

These central moments make it possible to assess the steepness of the temperature profile at the boundary of two neighbouring zones. In a sufficient distance from the boundary a steady state of the temperatures and thus also of the mobilities is established; this can, clearly, take place only in sufficiently long zones.

If, however, a zone 2 is placed between the zones 1 and 3, we have to take into account the mutual influencing of the temperature profiles of the non-neighbouring zones 1 and 3. The shorter is the central zone 2, the more is the shape of the temperature profile at the first interface affected by the temperature of the third zone, and conversely, the temperature distribution at the second interface is affected by the temperature of the first zone. When very short zones occur, the qualitative as well as quantitative detection can be difficult, since due to the temperature dependence of the mobilities, the detector response and the concentration of the component monitored may not attain their steady-state values along the axis. Eqs (*14a, b*), (*15a, b*), and (*20a, b*) are then no longer valid. At any rate, for a short zone of the length a, encompassed by two long zones, the heat balance according to Eq. (*4*) holds true. If we start from the assumption of a field intensity jump at the boundary, which is warranted as will be shown later, we arrive, analogously as in the preceding case, at the solution of the temperature profiles in the form

$$\vartheta_1 = \frac{\lambda_2 - \lambda_1}{\lambda_2} \{R \exp [\lambda_1(x - a)] + \exp (\lambda_1 x)\} \tag{29a}$$

$$\vartheta_2 = \frac{\lambda_2 - \lambda_1}{\lambda_2} R \exp [\lambda_1(x - a)] + \frac{\lambda_1}{\lambda_2 - \lambda_1} \exp (\lambda_2 x) + 1 \tag{29b}$$

$$\vartheta_3 = \frac{\lambda_1}{\lambda_2 - \lambda_1} \{\exp (\lambda_2 x) + R \exp [\lambda_2(x - a)]\} + R + 1 \tag{29c}$$

where

$$\vartheta_1 = [T_i - T_0 - QP_1]/[Q(P_2 - P_1)] \tag{30}$$

and

$$R = (P_3 - P_2)/(P_2 - P_1) . \tag{31}$$

In case that allowance is made for the temperature dependence of the mobilities, four constants appear in the solution:

$$\omega_1 = \tfrac{1}{2}\{m + [m^2 + 4\beta(1 + \alpha_1 QP_1^0)]^{1/2}\} \tag{32a}$$

$$\omega_2 = \tfrac{1}{2}\{m + [m^2 + 4\beta(1 + \alpha_2 QP_2^0)]^{1/2}\} \tag{32b}$$

$$\omega_3 = \tfrac{1}{2}\{m - [m^2 + 4\beta(1 + \alpha_2 QP_2^x)]^{1/2}\} \tag{32c}$$

$$\omega_4 = \tfrac{1}{2}\{m - [m^2 + 4\beta(1 + \alpha_3 QP_3^0)]^{1/2}\} . \tag{32d}$$

In the case of rapid isotachophoretic analyses the exponents $\omega_1 a$, $\omega_2 a$ are positive and much greater than the absolute values of the negative $\omega_3 a$ and $\omega_4 a$. The solution can be then simplified to[20]

$$\vartheta_1 = [\omega_3/(\omega_3 - \omega_1)] \exp(\omega_1 x) \tag{33a}$$

$$\vartheta_2 = \left[\frac{\omega_1}{\omega_3 - \omega_1}\frac{\omega_4 - \omega_3}{\omega_2 - \omega_4}\exp(\omega_3 a) - \frac{\omega_4}{\omega_2 - \omega_4} R\right]\{\exp[\omega_2(x - a)]\} + + \frac{\omega_1}{\omega_3 - \omega_1}\exp(\omega_3 a) + 1 \tag{33b}$$

$$\vartheta_3 = \left[\frac{\omega_1}{\omega_3 - \omega_1}\frac{\omega_2 - \omega_3}{\omega_2 - \omega_4}\exp(\omega_2 a) - \frac{\omega_2}{\omega_2 - \omega_4} R\right]\{\exp[\omega_4(x - a)]\} + + R + 1 . \tag{33c}$$

RESULTS AND DISCUSSION

For a description of the temperature behaviour at the zone boundary, the mutual significance of the temperature dependence of the conductivity and of the diffusion blurring of the boundary must be compared. It is necessary to decide, which of these two factors alters the profile shapes more and the neglecting of which introduces a greater error.

We shall first consider the influence of the width of the region, in which the electric field intensity changes continuously, on the shape of the profiles at the boundary of two long zones. For the modelling of the potential gradient at the boundary, the symmetrical case $g_1 = |g_2| = 0{\cdot}5$, $r_1 = |r_2| = 100\ \mathrm{cm}^{-1}$ was chosen. If the boundary

TABLE I

Dependence of the Second Central Moment μ_2 (10^{-2} cm^2) on the Migration Velocity and Cooling Efficiency of the Column for Different Diffusion Boundary Widths

v cm/min	$QS = 0{\cdot}3$		$QS = 0{\cdot}9$	
	$r \to \infty$	$r = 100$	$r \to \infty$	$r = 100$
0	0·360	0·425	1·085	1·105
4	1·06	1·08	7·372	7·384
8	3·16	3·18	26·229	26·249

width is defined as $D = |x_1| + |x_2|$, for which $\exp(r_1 x_1) = \exp(r_2 x_2) = 0{\cdot}01$, then the width $D = 0{\cdot}92$ mm corresponds to the chosen value of r. The actual boundary width is, in fact, considerably smaller[18,21]. In Table I, several values of the second central moment are given for various migration velocities and various products QS (the quotients representing the temperature rise with the volume power). From this table it can be seen that with the deteriorating cooling efficiency and growing migration velocity, the shapes of the profiles, calculated from Eqs (*15a, b*) and (*14a, b*), approach each other rapidly. From this it follows that in current experimental conditions, where great migration velocities are applied, allowance need not be made for the continuous character of the field intensity, and the assumption of a jump of the dissipated power at the boundary is justified.

Fig. 1 shows the dependence of the second central moment of the function $d\xi/dx$ on the migration velocity for different QS values. This dependence has been calculated from Eqs (*15a, b*) and (*28*). The shape of the curves is reminiscent of the experimental dependences of μ_2 on the migration velocity[7], the values, however, are lower. The difference is particularly due to the signal distortion during the passage through the column wall and the time course of heating of the thermocouple detector. The width of the temperature boundary increases similarly too.

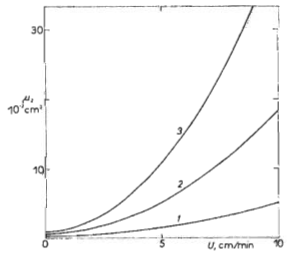

FIG. 1

Dependence of the Second Central Moment μ_2 of the Function $d\xi/dx$, Calculated from Eq. (*15a,b*), on the Migration Velocity for Different QS Values

QS [K cm^3 W^{-1}]: *1* 0·3, *2* 0·6, *3* 0·9.

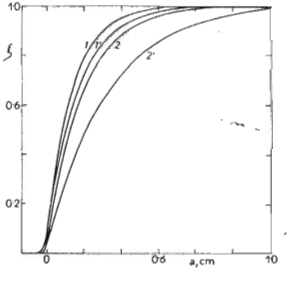

FIG. 2

Temperature Distribution at the Interface of Bromide and Iodate Zones with 0·005M-NaBr as the Leading Electrolyte, Calculated for the Model Neglecting Both the Temperature Dependence of the Mobilities and the Continuous Character of the Power at the Boundary (curves *1'*, *2'*), and for the Model in which Allowance is Made only for the Temperature Dependence of the Mobilities (curves *1*, *2*)

Driving current: *1*, *1'* 175 μA, *2*, *2'* 350 μA.

If, however, greater zone heating is applied, the temperature distribution must be calculated according to Eqs (*20a*, *b*), where the temperature dependence of the mobilities is not neglected. In fact, by neglecting the temperature dependence we would introduce a greater error than by approximating the continuous variations of the concentrations at the boundary by a jump function; the effect of the temperature dependence on the profile shape is considerable and favours the sharpening of the temperature profile. Fig. 2 shows the temperature distribution at the interface of zones $Br^- - IO_3^-$ (leading electrolyte 0·005M-NaBr) calculated from Eqs (*15a*, *b*) (curves *1'*, *2'*) and (*20a*, *b*) (curves *1*, *2*) for currents 175 μA (curves *1*, *1'*) and 350 μA (curves *2*, *2'*). The limiting power values in large distances from the interface were calculated by applying the procedure given in detail in ref.[8] for a rectangular cross section column described elsewhere[22], whose temperature parameters were $Q = 160$ K cm W^{-1}, $S = 0{\cdot}0024$ cm^2.

Fig. 3 depicts the potential gradient at the boundary, calculated under the assumption of the occurrence of the temperature profile according to Fig. 2. The actual potential gradient at the boundary will be somewhat lower, as the concentration diffusion at the boundary shows here up. That the decrease after the passage of the boundary (bromide – iodate) through the detector compartment is not so pronounced in reality, is documented by Fig. 4, where the passage of the $Br^- - IO_3^-$ interface is recorded. Additional causes of the difference between the actual and calculated detector response lie in the voltmeter and detector lags, which bring about a distortion of the signal at the boundary, and in the heating of the detector whose thermal capacity may differ from the environment. Despite the typical shape of the response, as given in

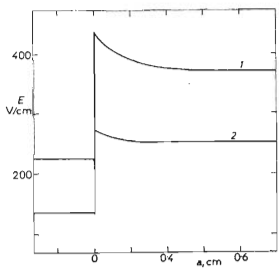

FIG. 3

Theoretical Profile of the Electric Field Intensity at the Bromide – Iodate Interface for the Driving Currents 350 (*1*) and 175 μA (*2*)

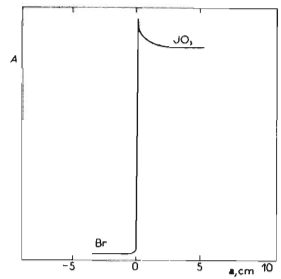

FIG. 4

Shape of the Record Obtained with a Potential Gradient Detector During the Passage of the Boundary $Br^- - IO_3^-$ at 350 μA

Figs 3 and 4, it is usual during the detection of a zone with fairly different temperatures. In the past, this effect was explained in terms of the gradual heating in the detection cell compartment[16], which naturally plays a role in columns in which the Q value varies appreciably near the detector cell.

During rapid separation of minor components, the non-neighbouring zones, whose mobilities differ appreciably and which are separated from each other by a short zone of the minor component, affect each other. In the minor component zone, a temperature gradient, and thus also an electric field intensity gradient, occur then along the whole zone length. As a consequence, the detector response to the minor component is not steady, the qualitative interpretation is therefore more difficult. Fig. 5 shows the temperature profiles calculated for the zone system bromide–bromate–iodate, bromate being the minor component and its zone length being variable in the range 0·2–1·2 cm in 0·2 cm steps. The temperature gradient is seen to be very steep (the difference between the temperatures at the two zone ends can be as high as 4°C). Unless the bromate zone is at least 1·2 cm long, its temperature does not attain its constant level. The temperature profile exhibits an inflexion at a temperature lower than the steady-state value occurring in a sufficiently long zone. A short bromate zone migrates thus in different temperature conditions as compared with a long zone. Thus the effective mobilities of the same substance in differently long zones are different owing to the different axial temperature profiles. From the qualitative analytical point of view, differently long zones of the same substance appear as zones of different substances.

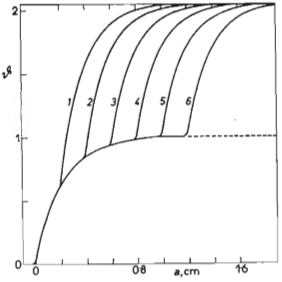

FIG. 5

Temperature Distribution in Bromide, Bromate, and Iodate Zones at 350 μA, Calculated by Means of Eq. (*33a–c*) for Bromate Zones of Different Lengths

a [cm]: *1* 0·2, *2* 0·4, *3* 0·6, *4* 0·8, *5* 1·0, *6* 1·2.

LIST OF SYMBOLS

C specific heat of the solution $J\,g^{-1}\,K^{-1}$
F_0 radial heat flux in a unit length of the column $W\,cm^{-1}\,s^{-1}$
H coefficient of heat transfer from the column wall surface into the surroundings $W\,cm^{-2}\,K^{-1}$
k_1 thermal conductivity coefficient of the solvent $W\,cm^{-1}\,K^{-1}$
k_2 thermal conductivity coefficient of the column material $W\,cm^{-1}\,K^{-1}$
P_i^0 power dissipated in the i-th zone in a large distance from the boundary $W\,cm^{-1}$
Q quotient of the increase of the mean temperature with the power dissipated in a unit length of the column $K\,cm\,W^{-1}$
R_1 inner diameter of the column cm
R_2 outer diameter of the column cm
S cross section of the column cm^2
T mean temperature in the zone K
U migration velocity $cm\,s^{-1}$
x coordinate along the column axis cm
α_i coefficient of the temperature dependence of the effective mobility in the i-th zone K^{-1}
μ_1 the first moment cm
μ_2 the second central moment cm^2
ϱ density of the solution $g\,cm^{-3}$
τ time s

REFERENCES

1. Kendall J.: Science *67*, 163 (1928).
2. Konstantinov B. P., Oshurkova O. V.: Zh. Tekh. Fiz. *37*, 1745 (1967).
3. Martin A. J. P., Everaerts F. M.: Anal. Chim. Acta *38*, 233 (1967).
4. Martin A. J. O., Everaerts F. M.: Proc. Soy. Soc., Sec. A *316*, 493 (1970).
5. Everaerts F. M.: *Thesis*. Technical University, Eindhoven 1968.
6. Vacík H., Zuska J.: J. Chromatogr. *91*, 795 (1974).
7. Ryšlavý Z., Vacík J., Zuska J.: J. Chromatogr. *114*, 315 (1975).
8. Boček P., Ryšlavý Z., Deml M., Janák J.: J. Chromatogr., in press.
9. Ryšlavý Z., Boček P., Deml M., Janák J.: J. Chromatogr. *114*, 17 (1977).
10. Ryšlavý Z.: Unpublished results.
11. Brown J. F., Hinckley J. O. N.: J. Chromatogr. *109*, 218 (1975).
12. Brown J. F., Hinckley J. O. N.: J. Chromatogr. *109*, 225 (1975).
13. Coxon M., Binder M. J.: J. Chromatogr. *101*, 1 (1974).
14. Coxon M., Binder M. J.: J. Chromatogr. *107*, 43 (1975).
15. Boček P., Ryšlavý Z., Deml M., Janák J.: This Journal *42*, 3382 (1977).
16. Verheggen Th. P. E. M., Mikkers F. E. P., Everaerts F. M.: J. Chromatogr. *132*, 205 (1977).
17. Carslaw H. S., Jaeger J. C.: *Conduction of Heat in Solids*. Clarendon Press, Oxford 1959.
18. Coxon M., Binder M. J.: J. Chromatogr. *95*, 133 (1974).
19. Brouwer G., Postema G. A.: J. Electrochem. Soc. *117*, 874 (1970).
20. Ryšlavý Z.: *Thesis*. Czechoslovak Academy of Sciences, Brno 1979.
21. Konstantinov B. P., Oshurkova O. V.: Dokl. Akad. Nauk SSSR *148*, 1110 (1963).
22. Boček P., Deml M., Janák J.: J. Chromatogr. *106*, 283 (1975).

Translated by P. Adámek.